Systematic study of synthesizing various heteroatom-substituted rhodamines from diaryl ether analogues

Fei Deng, Limin Liu, Wei Huang, Chunfang Huang, Qinglong Qiao, Zhaochao Xu

PII: S1386-1425(20)30444-3

DOI: https://doi.org/10.1016/j.saa.2020.118466

Reference: SAA 118466

To appear in: *Spectrochimica Acta Part A: Molecular and Biomolecular Spectroscopy*

Received date: 26 March 2020

Revised date: 8 May 2020

Accepted date: 9 May 2020

Please cite this article as: F. Deng, L. Liu, W. Huang, et al., Systematic study of synthesizing various heteroatom-substituted rhodamines from diaryl ether analogues, *Spectrochimica Acta Part A: Molecular and Biomolecular Spectroscopy* (2018), https://doi.org/10.1016/j.saa.2020.118466

Systematic study of synthesizing various heteroatom-substituted rhodamines from diaryl ether analogues

Fei Deng[a,b], Limin Liu[a,*], Wei Huang[a], Chunfang Huang[a], Qinglong Qiao[b,*], Zhaochao Xu[b,*]

[a]School of Chemistry and Chemical Engineering, Jinggangshan University, Ji'an, Jiangxi 343009, China.
[b]CAS Key Laboratory of Separation Science for Analytical Chemistry, Dalian Institute of Chemical Physics, Chinese Academy of Sciences, Dalian 116023, China.

*Corresponding authors
E-mail addresses: zcxu@dicp.ac.cn (Z. Xu); qqlqiao@dicp.ac.cn (Q. Qiao); llm24@126.com (L. Liu)

Abstract

The dye rhodamine, as the most popular scaffold to construct fluorescent labels and probes, has been explored extensively on its structure-fluorescence relationships. Particularly, the replacement of the oxygen atom in the 10th position with heteroatoms obtained various new rhodamines with improved photophysical properties, such as brightness, photostability, red-shifted emission and fluorogenicity. However, the applications of heteroatom-substituted rhodamines have been hindered by difficult synthetic routes. Herein, we explored the condensation strategy of diaryl ether analogues and *o*-tolualdehyde to synthesize various heteroatom-substituted rhodamines. We found that the electron property and steric effect in the rhodamine 10th position determined the synthetic yield. It's concluded that this condensation method was more suitable for the synthesis of heteroatom-substituted rhodamines with small or electron-donating groups like rhodamine, S-rhodamine and Si-rhodamine. We hope these results will benefit the design and synthesis of heteroatom-substituted rhodamines.

Keywords

Rhodamine; Heteroatom; Fluorescence; Friedel-Crafts reaction; Diaryl ether analogues

1. Introduction

The advance of fluorescence imaging is driving the revolution of fluorophores to get better brightness, photostability, large stokes shift, near-infrared (NIR) spectrum, and fluorogenicity [1-10]. Rhodamines, as the most popular scaffold in conventional confocal imaging, are among the best choices for these purposes through rational modification [11-13]. Recently, substituting the bridging oxygen atom of rhodamine with silicon atom has attracted great interests [14, 15]. The so-called Si-rhodamines red-shift the absorption and emission maximum into deep-red or NIR region, facilitating tissue penetration and mitigating auto fluorescence during in vivo imaging. Besides, the stronger electrophilic property of the 9th carbon atom in Si-rhodamine facilitate the

construction of functional compounds, such as fluorogenic dyes [16-18], blinking dyes [19-22] and fluorescent probes [23-26]. The success of Si-rhodamine also inspired the appearance of other heteroatom-substituted rhodamines, such as B-rhodamine [27], P-rhodamine [28-30] and Ge-rhodamine [31-33]. These heteroatom contained moieties in the rhodamine 10^{th} position not only tune the spectra, but also improve the photophysical properties, such as brightness and photostability [34, 35].

Rhodamine was traditionally synthesized through the Friedel-Crafts reactions of meta-aminophenol and phthalic anhydride (Scheme 1a). Unfortunately, this method resulted in a mixture of 5'- and 6'-regioisomers via use of a 3-functionalized anhydride as starting material. Latterly, an improved synthesis method was proposed by using the corresponding benzaldehydes as anhydride replacements [36]. Compared to traditional O-rhodamine, syntheses of Si-rhodamines were more complicated, including introducing silicon contained moiety and fusing the pendent rings (Scheme 1b). As shown in route 1, the key intermediate Si-anthrone was obtained through lithium-halogen exchange reaction followed by potassium permanganate oxidation. Subsequently, the arylmetal nucleophile was added to a Si-anthrone with the formation of Si-rhodamine [23, 31]. In addition to the long-step uses of active organometallic reagents, the yield from diarylmethane to Si-anthrone was usually low (~ 30%), thus increasing the difficulty in synthesis. Inspired by the improved method in O-rhodamine, route 2 was proposed. It partially solved the problems in route 1 through the condensation of diaryl silyl ether and benzaldehydes analogues [37]. However, the condensation conditions for Si-rhodamines were much harsher in temperature and concentration compared to O-rhodamine. As presented in route 3, transfering the diaryl silyl ether to electron-rich diarylmetal silyl ether would enable the milder synthesis [38, 39]. Besides, the diarylmetal silyl ether also connected diaryl silyl ether with Si-anthrone in route 4 [32].

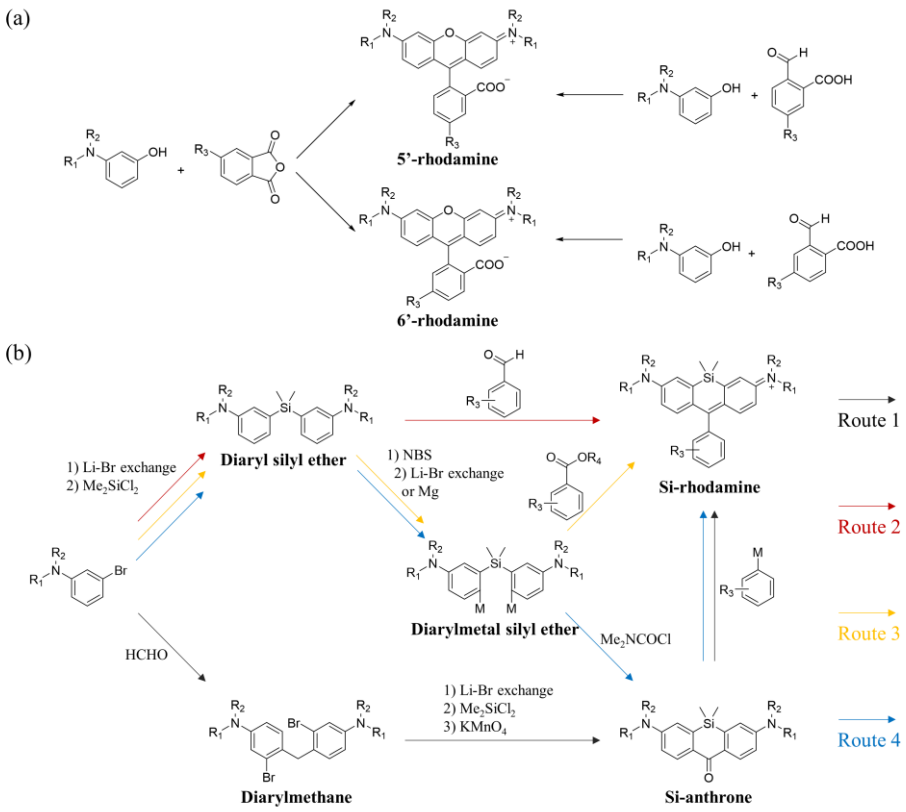

Scheme 1. Strategies for the synthesis of (a) O-rhodamines and (b) Si-rhodamines.

Due to the similarity in structures, these synthetic strategies for Si-rhodamine were applied to other heteroatom-substituted rhodamines. Most of the reported heteroatom-substituted rhodamines were synthesized according to the synthetic route 1 or 4, including S-rhodamine [40], Se-rhodamine [41], Te-rhodamine [42], C-rhodamine [43], Ge-rhodamine [31], P-rhodamine [30] and sulfone-rhodamine [44]. Besides, route 3 has also been reported to synthesize O-rhodamine, N-rhodamine and P-rhodamine [39, 45]. However, the application of route 2 has rarely been discussed. Considering the minimum synthesis steps and least organometallic reagents used, we aimed to investigate this cost-effective strategy in detail. As shown in Scheme 2, five heteroatom-substituted rhodamines with the spectra ranging from orange to NIR were synthesized through the condensation of diaryl ether analogues (**DAEA**s) and *o*-tolualdehyde. Our results indicated the synthetic yields were related to the substituted moiety in the rhodamine 10th position. It suggested that this is a priority synthetic route for O-rhodamine, S-rhodamine, Si-rhodamine, but not for P-rhodamine and sulfone-rhodamine.

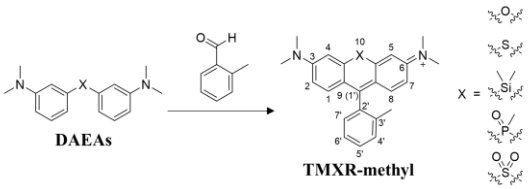

Scheme 2. Synthesis of **TMXR-methyl** through the condensation of **DAEA** and *o*-tolualdehyde.

2. Material and methods

2.1. Material and Instruments

Unless otherwise stated, all reagents and solvents for synthesis and detection were purchased from commercial suppliers and used without further purification. All water used was from a Millipore water purification system with a minimum resistivity of 18.0 MΩ·cm. Heteroatom-substituted rhodamines were purified by Waters PREP150 preparative HPLC (XSelect C18, 30 mm × 150 mm). ^{1}H NMR and ^{13}C NMR spectra were recorded on a Bruker 400 spectrometer, using TMS as an internal standard. Chemical shifts were given in ppm and coupling constants (*J*) in Hz. Mass spectrometry data were obtained with a HP1100LC/MSD mass spectrometer and a LC/Q-TOF MS spectrometer. UV-Vis absorption spectra were collected on an Agilent Cary60 UV-Vis Spectrophotometer. Fluorescence measurements were performed on an Agilent CARY Eclipse fluorescence spectrophotometer (Serial No. FL0812-M018).

*2.2. Synthesis of **DAEA-O***

This compound was synthesized according to the literature [39].^{1}H NMR (400 MHz, $CDCl_3$) δ 7.15 (t, *J* = 8.0 Hz, 2H), 6.50 – 6.42 (m, 4H), 6.35 (ddd, *J* = 8.1, 2.2, 0.9 Hz, 2H), 2.92 (s, 12H). MS (ESI) m/z: calcd. for$C_{16}H_{20}N_2O$ $[M+H]^+$ 257.1654, observed 257.1685.

*2.3. Synthesis of **DAEA-S***

The mixture of 3-iodide-*N*,*N*-diethylaniline (247 mg, 1 mmol), CuI (19 mg, 0.1 mmol), K_2CO_3 (138 mg, 1 mmol), $Na_2S{\cdot}9H_2O$ (144 mg, 0.6 mmol), and 2 mL DMF were stirred vigorously at 120 °C for 18 h under N_2. The resulting mixture was cooled to RT and diluted with EtOAc (50 mL). After washing with water (2 × 25 mL) and brine (25 mL), the organic layers dried over Na_2SO_4 and then concentrated under vacuum. The residue was purified by column chromatography to give product (103 mg, 76%). ^{1}H NMR (400 MHz, $CDCl_3$) δ 7.14 (t, *J* = 8.0 Hz, 2H), 6.81 – 6.72 (m, 2H), 6.69 (d, *J* = 7.6 Hz, 2H), 6.59 (dd, *J* = 8.4, 2.5 Hz, 2H), 2.90 (s, 12H). ^{13}C NMR (100 MHz, $CDCl_3$) δ 151.04, 136.44, 129.56, 119.05, 114.79, 111.20, 40.50. MS (ESI) m/z: calcd. for $C_{16}H_{20}N_2S$ $[M+H]^+$ 273.1425, observed 273.1433.

*2.4. Synthesis of **DAEA-Si***

This compound was synthesized according to the literature [38].^{1}H NMR (400 MHz, $CDCl_3$) δ 7.26 – 7.19 (m, 2H), 6.93 (d, *J* = 2.7 Hz, 2H), 6.91 (d, *J* = 7.1 Hz, 2H), 6.76 (dd, *J* = 8.2, 2.5 Hz, 2H), 2.92 (s, 12H), 0.56 (s, 6H). MS (ESI) m/z: calcd for $C_{18}H_{26}N_2Si$ $[M+H]^+$ 299.1944, observed 299.1965.

*2.5. Synthesis of Compound **1***

This compound was synthesized according to the literature [28].^{1}H NMR (400 MHz, DMSO-d_6) δ 8.62 (d, *J* = 12.0 Hz, 2H), 8.42 (d, *J* = 8.1 Hz, 2H), 8.30 (dd, *J* = 10.9, 7.7 Hz, 2H), 7.86 (td, *J* =

8.0, 2.8 Hz, 2H), 2.31 (d, *J* = 14.1 Hz, 3H).

*2.6. Synthesis of Compound **2***

This compound was synthesized according to the literature [28].^{1}H NMR (400 MHz, DMSO-d_6) δ 7.12 (td, *J* = 7.6, 3.6 Hz, 2H), 6.89 (d, *J* = 13.1 Hz, 2H), 6.79 (dd, *J* = 10.9, 7.7 Hz, 2H), 6.68 (d, *J* = 7.6 Hz, 2H), 5.33 (s, 4H), 1.82 (d, *J* = 13.1 Hz, 3H).

*2.7. Synthesis of **DAEA-PO***

To a suspension of compound **2** (0.99 g, 4 mmol) and K_2CO_3 (4.42 g, 32 mmol) in DMF (40 mL) added CH_3I (2.0 mL, 32 mmol). The mixture was stirred for 12 h at 100℃. The reaction mixture was cooled to RT and remove the solvent under vacuo. The residue was extracted with 100 mL CH_2Cl_2 and washed with water (2 x 50 mL) and brine (50 mL). After drying over Na_2SO_4, the organic layers were concentrated under vacuum and purified by column chromatography to give product (0.93 g, 77%). ^{1}H NMR (400 MHz, $CDCl_3$) δ 7.33 – 7.24 (m, 2H), 7.19 (dt, *J* = 13.9, 1.9 Hz, 2H), 6.92 (dd, *J* = 11.5, 7.4 Hz, 2H), 6.87 – 6.78 (m, 2H), 2.97 (s, 12H), 1.97 (d, *J* = 13.1 Hz, 3H). ^{13}C NMR (100 MHz, $CDCl_3$) δ 150.39, 135.27, 134.28, 129.21, 129.07, 117.96, 115.23, 114.21, 114.11, 40.46, 17.21, 16.49. MS (ESI) m/z: calcd. for $C_{17}H_{23}N_2OP$ $[M+H]^+$ 303.1626, observed 303.1622.

*2.8. Synthesis of Compound **3***

To a stirred solution of diphenyl sulfone (2.18 g, 10 mmol) in 50 mL sulfuric acid, 1.73 mL nitric acid was added slowly over 10 min at r.t. After stirring for 24 h, the mixture was poured on to ice, deposit was filtered and washed with saturated $NaHCO_3$ and brine, successively. Then the solid was dried to afford product (2.99 g, 97%). ^{1}H NMR (400 MHz, DMSO-d_6) δ 8.74 (t, *J* = 2.1 Hz, 2H), 8.58 – 8.50 (m, 4H), 7.96 (t, *J* = 8.1 Hz, 2H).^{13}C NMR (100 MHz, DMSO-d_6) δ 148.71, 141.68, 134.47, 132.54, 129.45, 123.19.

*2.9. Synthesis of Compound **4***

To a solution of Pd/C (0.16 g, 10% Pd/C) in 20 mL MeOH, compound **3** (1.54 g, 5 mmol) was added. The mixture was stirred under the atmosphere of hydrogen at room temperature for 12 h. Then the solution was filtered and concentrated under vacuum to afford the product (1.18 g, 95%). ^{1}H NMR (400 MHz, DMSO-d_6) δ 7.21 (t, *J* = 7.9 Hz, 2H), 7.03 (t, *J* = 1.9 Hz, 2H), 6.95 (d, *J* = 7.7 Hz, 2H), 6.77 (dd, *J* = 8.0, 1.6 Hz, 2H), 5.67 (s, 4H). ^{13}C NMR (100 MHz, DMSO-d_6) δ 150.13, 142.49, 130.37, 118.47, 114.09, 111.63. MS (ESI) m/z: calcd. for $C_{12}H_{12}N_2O_2S$ $[M+H]^+$ 249.0698, observed 249.0696.

*2.10. Synthesis of **DAEA-SO$_2$***

To a suspension of compound **4** (1.24 g, 5 mmol) and K_2CO_3 (5.53 g, 40 mmol) in DMF (50 mL) added CH_3I (2.5 mL, 40 mmol). The mixture was stirred for 12 h at 100℃. The reaction mixture

was cooled to RT and remove the solvent under vacuo. The residue was extracted with 100 mL CH_2Cl_2 and washed with water (2 x 50 mL) and brine (50 mL). After drying over Na_2SO_4, the organic layers were concentrated under vacuum and purified by column chromatography to give product (1.05 g, 69%). ^{1}H NMR (400 MHz, $CDCl_3$) δ 7.25 (dt, *J* = 19.7, 7.8 Hz, 6H), 6.80 (dd, *J* = 8.2, 2.0 Hz, 2H), 2.97 (s, 12H). ^{13}C NMR (100 MHz, $CDCl_3$) δ 150.57, 142.45, 129.76, 116.10, 114.84, 110.19, 40.33. MS (ESI) m/z: calcd. for $C_{16}H_{20}N_2O_2S$ $[M+H]^+$ 305.1324, observed 305.1319.

2.11. General method to synthesize heteroatom-substituted rhodamines

The corresponding **DAEA** (0.5 mmol), *o*-tolualdehyde (300 mg, 2.5 mmol) and *p*-TsOH·H_2O (95 mg, 0.5 mmol) were mixed in a sealable pressure tube. The tube was sealed tightly and heated at 140 °C for 8 h. After cooling to room temperature, the mixture was diluted with 2 mL MeOH, then added chloranil (123 mg, 0.5 mmol) and stirred for 2 h. After filtration and removal of the solvent, the residue was purified roughly by column chromatography on silica gel. An analytically pure sample was obtained through further purification by preparative HPLC (30–90% MeOH/H_2O + 0.5% v/v TFA). **TMOR-methyl** (191 mg, 81%).^{1}H NMR (400 MHz, MeOD) δ 7.62 – 7.43 (m, 3H), 7.26 (dd, *J* = 7.6, 1.3 Hz, 1H), 7.20 (d, *J* = 9.5 Hz, 2H), 7.09 (dd, *J* = 9.5, 2.4 Hz, 2H), 6.96 (d, *J* = 2.4 Hz, 2H), 3.32 (s, 12H), 2.05 (s, 3H). ^{13}C NMR (100 MHz, MeOD) δ 158.26, 157.81, 157.68, 135.83, 131.77, 130.95, 130.49, 129.89, 128.69, 125.89, 114.35, 113.33, 96.19, 39.59, 18.24. MS (ESI) m/z: calcd. for $C_{24}H_{25}N_2O^+$ $[M]^+$ 357.1961, observed 357.1920. **TMSR-methyl** (187 mg, 77%).^{1}H NMR (400 MHz, MeOD) δ 7.51 (tt, *J* = 20.1, 7.4 Hz, 3H), 7.34 (dd, *J* = 10.8, 6.1 Hz, 4H), 7.20 (d, *J* = 7.5 Hz, 1H), 7.11 (dd, *J* = 9.7, 2.6 Hz, 2H), 3.30 (s, 12H), 1.97 (s, 3H). ^{13}C NMR (100 MHz, MeOD) δ 159.89, 153.92, 144.33, 135.83, 135.35, 135.32, 130.36, 129.44, 128.79, 125.96, 118.44, 115.55, 105.41, 39.32, 18.02. MS (ESI) m/z: calcd. for $C_{24}H_{25}N_2S^+$ $[M]^+$ 373.1733, observed 373.1733. **TMSiR-methyl** (73 mg, 28%). ^{1}H NMR (400 MHz, MeOD) δ 7.41 (ddd, *J* = 17.3, 11.8, 5.1 Hz, 1H), 7.18 – 7.01 (m, 1H), 6.77 (dd, *J* = 9.6, 2.8 Hz, 1H), 3.34 (s, 3H), 2.03 (s, 1H), 0.60 (d, *J* = 6.9 Hz, 1H). MS (ESI) m/z: calcd. for $C_{26}H_{31}N_2Si^+$ $[M]^+$ 399.2251, observed 399.2236. **TMPOR-methyl** (10 mg, 4%). ^{1}H NMR (400 MHz, MeOD) δ 7.78 (dd, *J* = 15.9, 2.7 Hz, 2H), 7.53 (t, *J* = 7.5 Hz, 1H), 7.44 (dd, *J* = 16.3, 8.0 Hz, 2H), 7.27 – 7.09 (m, 3H), 6.97 (dd, *J* = 9.7, 2.7 Hz, 2H), 3.46 (s, 12H), 2.15 – 1.97 (m, 6H). ^{13}C NMR (100 MHz, MeOD) δ 164.01, 163.94, 155.40, 155.27, 139.93, 139.91, 139.85, 139.82, 138.88, 137.96, 136.01, 135.82, 135.52, 130.30, 130.17, 129.42, 129.39, 128.22, 125.74, 125.62, 122.57, 122.49, 122.41, 119.11, 119.03, 115.41, 40.09, 18.17, 18.02. MS (ESI) m/z: calcd. for $C_{25}H_{28}N_2OP^+$ $[M]^+$ 403.1934, observed 403.1939. **TMSO$_2$R-methyl** (1 mg, 0.4%). ^{1}H NMR (400 MHz, MeOD) δ 7.78 (t, *J* = 2.3 Hz, 2H), 7.58 – 7.38 (m, 3H), 7.22 (d, *J* = 7.5 Hz, 1H), 7.11 (dd, *J* = 9.6, 1.6 Hz, 2H), 6.98 (ddd, *J* = 9.6, 2.6, 1.3 Hz, 2H), 3.46 (s, 12H), 2.10 (s, 3H). ^{13}C NMR (100 MHz, MeOD) δ 159.72, 155.97, 144.34, 138.66, 136.03, 133.91, 130.45, 129.84, 128.88, 125.84, 118.93, 115.59, 112.02, 40.52, 18.09. MS (ESI) m/z: calcd. for $C_{24}H_{25}N_2O_2S^+$ $[M]^+$ 405.1631, observed 405.1632.

2.12. Computational methods

Geometry optimizations were performed at the B3LYP/6-31G level of theory, implemented in the Gaussian 09 program [46]. Next, the molecular electrostatic potentials were generated using

Multiwfn (version 3.7) [47] and VMD (version 1.9.3) [48].

3. Results and discussion

*3.1. Design and synthesis of **DAEA**s*

As the key intermediate to construct heteroatom-substituted rhodamines through the condensation reaction, we initially investigated the synthesis of **DAEA**s (Scheme 3). The diaryl ether **DAEA-O** was prepared through Ullmann reaction according to the previous method [39]. For diaryl sulfides **DAEA-S**, copper-catalyzed carbon-sulfur bond formation was applied. Although the aryl bromides could hardly react with $Na_2S{\cdot}9H_2O$ under the catalyzation of CuI, S-arylation through aryl iodides was in excellent yields. The synthesis of diaryl silyl ether have been detailedly described in previous reports [37, 38]. We used the Li/Br-exchange with *n*-BuLi and added dichlorodimethylsilane to afford **DAEA-Si** successfully. **DAEA-PO** containing P(=O)Me moiety was synthesized according to the similar procedure reported by Wang [28]. **DAEA-SO_2**, as the sulfone contained diaryl ether analogues, we originally intended to synthesize with reference to **DAEA-Si**. Unfortunately, the addition of sulfuryl chloride after Li/Br-exchange failed to afford **DAEA-SO_2**. Realizing diphenyl sulfone was commercially available, we decided to synthesize **DAEA-SO_2** with the procedure of introducing *N*,*N*-dimethyl. Similar to **DAEA-PO**, the specific steps included nitration, reduction, and alkylation.

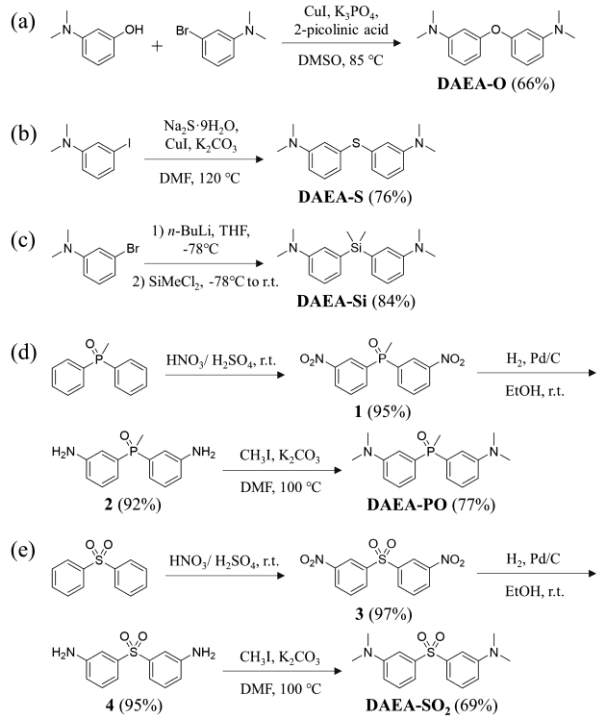

Scheme 3. Synthesis of **DAEA**s.

3.2. Design and synthesis of heteroatom-substituted rhodamines

With these **DAEA**s in hand, we further investigated the key cyclization step to form the heteroatom-substituted rhodamines. The condensation reactions of diaryl silyl ether and benzaldehydes analogues have been discussed in detail by Wang [28, 37]. We applied the optimized condition directly to synthesize the heteroatom-substituted rhodamines. Diaryl ether analogues condensed with 5.0 equivalent of *o*-tolualdehyde in the presence of the catalyst of *p*-toluenesulfonic acid. After 8h reaction at 140 ℃ in sealed tube, the condensed product was further oxidized with chloranil to heteroatom-substituted rhodamine. As shown in Scheme 4, **DAEA-O** and **DAEA-S** provided target products **TMOR-methyl** and **TMSR-methyl** with 81% and 77% isolated yields, respectively. However, the condensation of **DASE-Si** and *o*-tolualdehyde afforded a modest yield of **TMSiR-methyl** (28%). As for **DAEA-PO** and **DAEA-SO_2**, the same condensation condition could hardly provide target products **TMPOR-methyl** and **TMSO_2R-methyl**, with only 4% and 0.4% isolated yields. In the condensation process, bis-nucleophilic **DAEA**s were anticipated to attack twice to the electron-poor *o*-tolualdehyde and form the central C−C bonds of the dyes. We speculated the substituted moieties influenced the nucleophilic properties of **DAEA**s and resulted the difference in reaction yields.

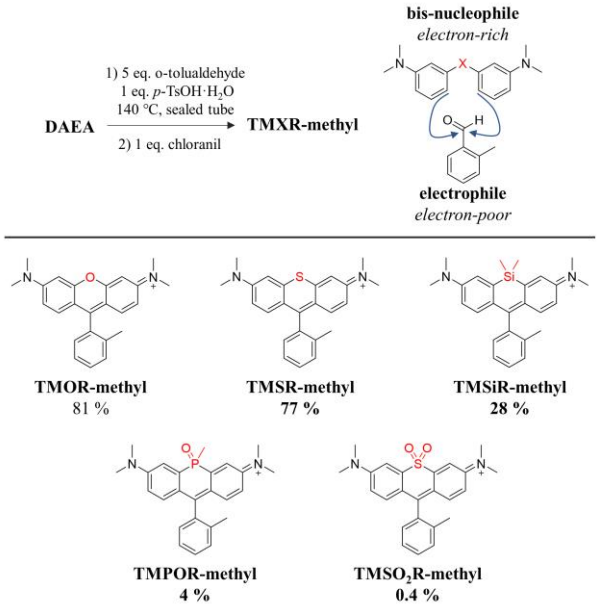

Scheme 4. Synthesis of **TMXR-methyl**.

3.3. Theoretical calculations

To further get insight into the relationship between the substituted moieties and reaction yields, we carried out theoretical calculations on **DAEA**s. C4 and C8, as the unsubstituted and electron-richest sites on each aromatic ring, were calculated to attack the electron-poor *o*-tolualdehyde and form the central C−C bonds of the dyes (Fig. 1 and Table S1-5). Specifically, the calculated electrostatic potential of C4 and C8 in **DAEA-O** were -20.82024 and -20.79005 kcal/mol respectively (Table 1). These values were slightly smaller than **DAEA-S** (-19.26014 and -20.76527 kcal/mol), which indicated the stronger nucleophilic ability and higher reaction yield in **DAEA-O**. Interestingly, **DAEA-Si** with lower reaction yield possessed much lower electrostatic

potentials (-20.38024 and -22.93891 kcal/mol for C4 and C8 respectively) compared to **DAEA-O** and **DAEA-S**. We attributed it to the steric effect. The substituted moiety in **DAEA-Si** was much larger than **DAEA-O** and **DAEA-S**, which hindered the nucleophilic reaction. As for **DAEA-PO** and **DAEA-SO$_2$**, the steric effects of P(=O)Me and SO_2 were similar to $Si(Me)_2$ in **DAEA-Si**. Besides, the strong electron-withdrawing properties of P(=O)Me and SO_2 resulted much higher electrostatic potentials in C4 and C8. These reasons prevented the nucleophilic reaction in **DAEA-PO** and **DAEA-SO$_2$**.

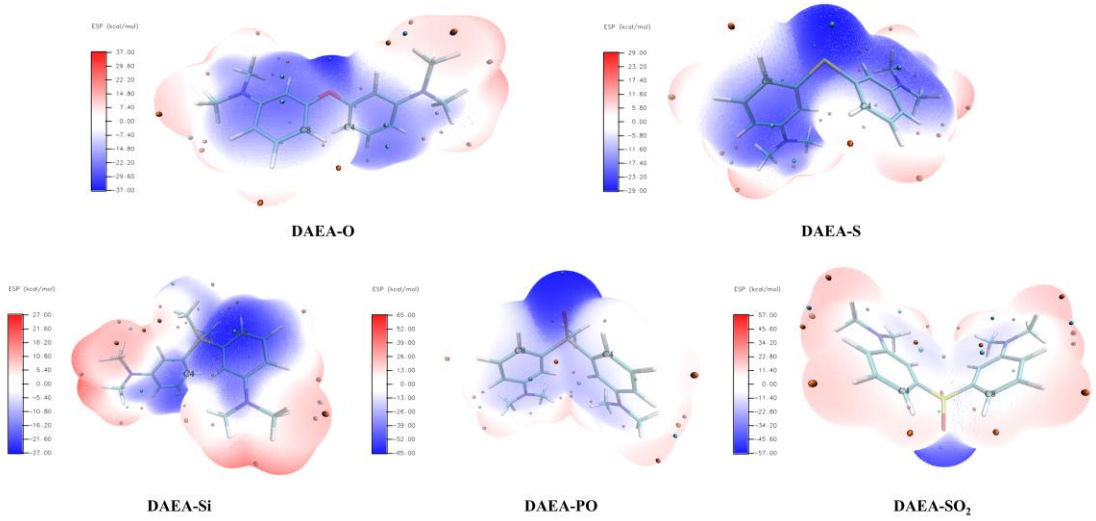

Fig. 1. Electrostatic potential surfaces of **DAEA**s.

Table 1. Electrostatic potential on C4 and C8 of **DAEA**s.

Compound	Atom	Electrostatic potential (kcal/mol)
DAEA-O	C4	-20.82024
	C8	-20.79005
DAEA-S	C4	-19.26014
	C8	-20.76527
DAEA-Si	C4	-20.38024
	C8	-22.93891
DAEA-PO	C4	-19.86078
	C8	-19.85955
DAEA-SO$_2$	C4	-13.58788
	C8	-13.58662

3.4. Photophysical properties of heteroatom-substituted rhodamines

Fig. 2 shows the absorption and fluorescence spectra of the heteroatom-substituted rhodamines synthesized in this work. Compared to **TMOR-methyl** and **TMSR-methyl**, the electron-donating property and σ*–π* conjugation of $SiMe_2$ red-shifted the absorption and fluorescence of

TMSiR-methyl [28, 44]. Furthermore, **TMPOR-methyl** and **TMSO$_2$R-methyl** possessing electron-withdrawing moieties displayed much more red-shifted spectra [44]. The specific photophysical properties of the dyes in aqueous solution were provided in Table 2.

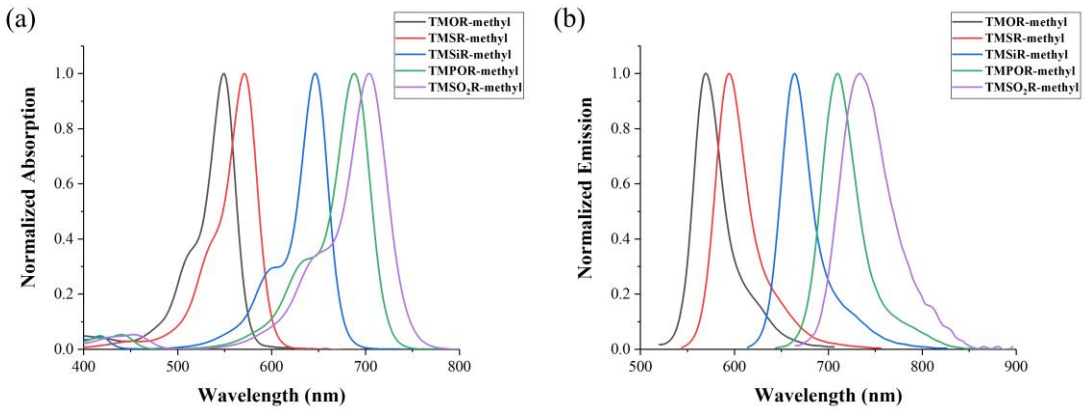

Fig. 2. (a) Absorption and (b) emission spectra of various heteroatom-substituted rhodamines.

Table 2. Photophysical properties of heteroatom-substituted rhodamines.[a]

Dye	λ_{abs} (nm)	ε (M^{-1} cm^{-1}× 10^5)	λ_{flu} (nm)	Φ_f
TMOR-methyl	549	0.72	570	0.31[b]
TMSR-methyl	571	0.61	592	0.33[c]
TMSiR-methyl	647	1.10	661	0.31[d]
TMPOR-methyl	688	0.98	709	0.16[e]
TMSO$_2$R-methyl	703	0.62	734	0.06[e]

[a] Measured in PBS (20 mM, pH 7.4).

[b] This value was taken from ref 27.

[c] Determinedusing R101 as standard (Φ_f = 0.91 in ethanol).

[d] This value was taken from ref 31.

[e] Determinedusing SiR700 as standard (Φ_f = 0.12 in PBS).

4. Conclusion

In summary, we have synthesized a series of heteroatom-substituted rhodamines through the condensation of **DAEA**s and *o*-tolualdehyde. The electron-rich C4 and C8 in **DAEA**s were anticipated to attack the electron-poor *o*-tolualdehyde and form the central C−C bonds of rhodamine. The electron-withdrawing substituted moieties in **DAEA**s decreased the nucleophilic ability of reaction sites and resulted the poor yields. Besides, the large substituted moieties in **DAEA**s hindered the reaction and further decreased yields. Moreover, the spectra of these rhodamines were determined by the substituted moiety in the 10th position. We hoped these results will benefit the design and synthesis of heteroatom-substituted rhodamines.

Acknowledgments

We acknowledge the financial support from National Natural Science Foundation of China (21765011, 21878286, 21908216) and Department of Education of Jiangxi Province (GJJ190567).

References

[1] G.T. Dempsey, J.C. Vaughan, K.H. Chen, M. Bates, X. Zhuang, Evaluation of fluorophores for optimal performance in localization-based super-resolution imaging, Nat. Meth. 8 (2011) 1027-1036.

[2] R. Sharma, M. Singh, R. Sharma, Recent advances in STED and RESOLFT super-resolution imaging techniques, Spectrochim. Acta A 231 (2020) 117715.

[3] M.V. Sednev, V.N. Belov, S.W. Hell, Fluorescent dyes with large Stokes shifts for super-resolution optical microscopy of biological objects: a review, Methods Appl. Fluores. 3 (2015) 042004.

[4] L.D. Lavis, Chemistry is dead. Long live chemistry!, Biochemistry 56 (2017) 5165-5170.

[5] L. Zhou, L. Xie, C. Liu, Y. Xiao, New trends of molecular probes based on the fluorophore 4-amino-1, 8-naphthalimide, Chin. Chem. Lett. 30 (2019) 1799-1808.

[6] L. Li, Y. Chen, W. Chen, Y. Tan, H. Chen, J. Yin, Photodynamic therapy based on organic small molecular fluorescent dyes, Chin. Chem. Lett. 30 (2019) 1689-1703.

[7] S. Long, Q. Qiao, L. Miao, Z. Xu, A self-assembly/disassembly two-photo ratiometric fluorogenic probe for bacteria imaging, Chin. Chem. Lett. 30 (2019) 573-576.

[8] F. Deng, L. Liu, Q. Qiao, C. Huang, L. Miao, Z. Xu, A general strategy to develop cell membrane fluorescent probes with location-and target-specific fluorogenicities: a case of a Zn^{2+} probe with cellular selectivity, Chem. Commun. 55 (2019) 15045-15048.

[9] C. Wang, Q. Qiao, W. Chi, J. Chen, W. Liu, D. Tan, S. McKechnie, D. Lyu, X.F. Jiang, W. Zhou, N. Xu, Q. Zhang, Z. Xu, X. Liu, Quantitative design of bright fluorophores and AIEgens by the accurate prediction of twisted intramolecular charge transfer (TICT), Angew. Chem. Int. Ed. 59 (2020) 13713–13719.

[10] F. Deng, S. Long, Q. Qiao, Z. Xu, The environmental-sensitivity of a fluorescent ZTRS-Cd(II) complex was applied to discriminate different types of surfactants and determine their CMC values, Chem. Commun. 54 (2018) 6157-6160.

[11] L.D. Lavis, Teaching old dyes new tricks: biological probes built from fluoresceins and rhodamines, Annu. Rev. Biochem. 86 (2017) 825-843.

[12] L. Wang, W. Du, Z. Hu, K. Uvdal, L. Li, W. Huang, Hybrid rhodamine fluorophores in the visible/NIR region for biological imaging, Angew. Chem. Int. Ed. 58 (2019) 14026-14043.

[13] Q. Qi, W. Chi, Y. Li, Q. Qiao, J. Chen, L. Miao, Y. Zhang, J. Li, W. Ji, T. Xu, X. Liu, J. Yoon, Z. Xu, A H-bond strategy to develop acid-resistant photoswitchable rhodamine spirolactams for super-resolution single-molecule localization microscopy, Chem. Sci. 10 (2019) 4914-4922.

[14] Y. Koide, Y. Urano, K. Hanaoka, W. Piao, M. Kusakabe, N. Saito, T. Terai, T. Okabe, T. Nagano, Development of NIR fluorescent dyes based on Si-rhodamine for in vivo imaging, J. Am. Chem. Soc. 134 (2012) 5029-5031.

[15] T. Ikeno, T. Nagano, K. Hanaoka, Silicon-substituted xanthene dyes and their unique photophysical properties for fluorescent probes, Chem. Asian J. 12 (2017) 1435-1446.

[16] G. Lukinavicius, K. Umezawa, N. Olivier, A. Honigmann, G.Y. Yang, T. Plass, V. Mueller, L. Reymond, I.R. Correa, Z.G. Luo, C. Schultz, E.A. Lemke, P. Heppenstall, C. Eggeling, S. Manley, K. Johnsson, A near-infrared fluorophore for live-cell super-resolution microscopy of cellular proteins, Nat. Chem. 5 (2013) 132-139.

[17] G. Lukinavicius, L. Reymond, K. Umezawa, O. Sallin, E. D'Este, F. Gottfert, H. Ta, S.W. Hell, Y. Urano, K. Johnsson, Fluorogenic probes for multicolor imaging in living cells, J. Am. Chem. Soc. 138 (2016) 9365-9368.

[18] J.B. Grimm, A.K. Muthusamy, Y. Liang, T.A. Brown, W.C. Lemon, R. Patel, R. Lu, J.J. Macklin, P.J. Keller, N. Ji, L.D. Lavis, A general method to fine-tune fluorophores for live-cell and in vivo imaging, Nat. Meth. 14 (2017) 987-994.

[19] S.N. Uno, M. Kamiya, T. Yoshihara, K. Sugawara, K. Okabe, M.C. Tarhan, H. Fujita, T. Funatsu, Y. Okada, S. Tobita, Y. Urano, A spontaneously blinking fluorophore based on intramolecular spirocyclization for live-cell super-resolution imaging, Nat. Chem. 6 (2014) 681-689.

[20] H. Takakura, Y.D. Zhang, R.S. Erdmann, A.D. Thompson, Y. Lin, B. McNellis, F. Rivera-Molina, S.N. Uno, M. Kamiya, Y. Urano, J.E. Rothman, J. Bewersdorf, A. Schepartz, D. Toomre, Long time-lapse nanoscopy with spontaneously blinking membrane probes, Nat. Biotechnol. 35 (2017) 773-780.

[21] S. Uno, M. Kamiya, A. Morozumi, Y. Urano, A green-light-emitting, spontaneously blinking fluorophore based on intramolecular spirocyclization for dual-colour super-resolution imaging, Chem. Commun. 54 (2018) 102-105.

[22] Q. Zheng, A.X. Ayala, I. Chung, A.V. Weigel, A. Ranjan, N. Falco, J.B. Grimm, A.N. Tkachuk, C. Wu, J. Lippincott-Schwartz, Rational design of fluorogenic and spontaneously blinking labels for super-resolution imaging, ACS Cent. Sci. 5 (2019) 1602-1613.

[23] K. Hanaoka, Y. Kagami, W. Piao, T. Myochin, K. Numasawa, Y. Kuriki, T. Ikeno, T. Ueno, T. Komatsu, T. Terai, Synthesis of unsymmetrical Si-rhodamine fluorophores and application to a far-red to near-infrared fluorescence probe for hypoxia, Chem. Commun. 54 (2018) 6939-6942.

[24] J. Wang, D. Cheng, L. Zhu, P. Wang, H.-W. Liu, M. Chen, L. Yuan, X.-B. Zhang, Engineering dithiobenzoic acid lactone-decorated Si-rhodamine as a highly selective near-infrared HOCl fluorescent probe for imaging drug-induced acute nephrotoxicity, Chem. Commun. 55 (2019) 10916-10919.

[25] J. Tang, Q. Li, Z. Guo, W. Zhu, A fast-response and highly specific Si-Rhodamine probe for endogenous peroxynitrite detection in living cells, Org. Biomol. Chem. 17 (2019) 1875-1880.

[26] M. Li, C. Wang, T. Wang, M. Fan, N. Wang, D. Ma, T. Hu, X. Cui, Asymmetric Si-rhodamine scaffold: rational design of pH-durable protease-activated NIR probes in vivo, Chem. Commun. 56 (2020) 2455-2458.

[27] X.Q. Zhou, L. Lesiak, R. Lai, J.R. Beck, J. Zhao, C.G. Elowsky, H. Li, C.I. Stains, Chemoselective alteration of fluorophore scaffolds as a strategy for the development of ratiometric chemodosimeters, Angew. Chem. Int. Ed. 56 (2017) 4197-4200.

[28] X.Y. Chai, X.Y. Cui, B.G. Wang, F. Yang, Y. Cai, Q.Y. Wu, T. Wang, Near-infrared phosphorus-substituted rhodamine with emission wavelength above 700 nm for bioimaging, Chem. Euro. J. 21 (2015) 16754-16758.

[29] X.Q. Zhou, R. Lai, J.R. Beck, H. Li, C.I. Stains, Nebraska red: a phosphinate-based near-infrared fluorophore scaffold for chemical biology applications, Chem. Commun. 52 (2016) 12290-12293.

[30] M. Grzybowski, M. Taki, K. Senda, Y. Sato, T. Ariyoshi, Y. Okada, R. Kawakami, T. Imamura, S. Yamaguchi, A highly photostable near- infrared labeling agent based on a phospha- rhodamine for long- term and deep imaging, Angew. Chem. Int. Ed. 57 (2018) 10137-10141.

[31] Y. Koide, Y. Urano, K. Hanaoka, T. Terai, T. Nagano, Evolution of group 14 rhodamines as platforms for near-infrared fluorescence probes utilizing photoinduced electron transfer, ACS Chem. Biol. 6 (2011) 600-608.

[32] A.N. Butkevich, V.N. Belov, K. Kolmakov, V.V. Sokolov, H. Shojaei, S.C. Sidenstein, D. Kamin, J. Matthias, R. Vlijm, J. Engelhardt, S.W. Hell, Hydroxylated fluorescent dyes for live-cell labeling: synthesis, spectra and super-resolution STED, Chem. Euro. J. 23 (2017) 12114-12119.

[33] Y. Koide, R. Kojima, K. Hanaoka, K. Numasawa, T. Komatsu, T. Nagano, H. Kobayashi, Y. Urano, Design strategy for germanium-rhodamine based pH-activatable near-infrared fluorescence probes suitable for biological applications, Commun. Chem. 2 (2019) 94.

[34] M. Li, Y. Li, X. Wang, X. Cui, T. Wang, Synthesis and application of near-infrared substituted rhodamines, Chin. Chem. Lett. 30 (2019) 1682-1688.

[35] F. Deng, Z. Xu, Heteroatom-substituted rhodamine dyes: Structure and spectroscopic properties, Chin. Chem. Lett. 30 (2019) 1667-1681.

[36] G. Mudd, I.P. Pi, N. Fethers, P.G. Dodd, O.R. Barbeau, M. Auer, A general synthetic route to isomerically pure functionalized rhodamine dyes, Methods Appl. Fluores. 3 (2015) 045002.

[37] B.G. Wang, X.Y. Chai, W.W. Zhu, T. Wang, Q.Y. Wu, A general approach to spirolactonized Si-rhodamines, Chem. Commun. 50 (2014) 14374-14377.

[38] J.B. Grimm, T.A. Brown, A.N. Tkachuk, L.D. Lavis, General synthetic method for Si-fluoresceins and Si-rhodamines, ACS Cent. Sci. 3 (2017) 975-985.

[39] C. Fischer, C. Sparr, Direct transformation of esters into heterocyclic fluorophores, Angew. Chem. Int. Ed. 57 (2018) 2436-2440.

[40] M.R. Detty, P.N. Prasad, D.J. Donnelly, T. Ohulchanskyy, S.L. Gibson, R. Hilf, Synthesis, properties, and photodynamic properties in vitro of heavy-chalcogen analogues of tetramethylrosamine, Bioorg. Med. Chem. 12 (2004) 2537-2544.

[41] W. Piao, K. Hanaoka, T. Fujisawa, S. Takeuchi, T. Komatsu, T. Ueno, T. Terai, T. Tahara, T. Nagano, Y. Urano, Development of an azo-based photosensitizer activated under mild hypoxia for photodynamic therapy, J. Am. Chem. Soc. 139 (2017) 13713-13719.

[42] Y. Koide, M. Kawaguchi, Y. Urano, K. Hanaoka, T. Komatsu, M. Abo, T. Terai, T. Nagano, A reversible near-infrared fluorescence probe for reactive oxygen species based on Te–rhodamine, Chem. Commun. 48 (2012) 3091-3093.

[43] K. Kolmakov, V.N. Belov, C.A. Wurm, B. Harke, M. Leutenegger, C. Eggeling, S.W. Hell, A versatile route to red-emitting carbopyronine dyes for optical microscopy and nanoscopy, Eur. J. Org. Chem. 2010 (2010) 3593-3610.

[44] J. Liu, Y.Q. Sung, H.X. Zhang, H.P. Shi, Y.W. Shi, W. Guo, Sulfone-rhodamines: a new class of near-infrared fluorescent dyes for bioimaging, ACS Appl. Mater. Interfaces 8 (2016)

22953-22962.

[45] M. Sauer, V. Nasufovic, H.-D. Arndt, I. Vilotijevic, Robust synthesis of NIR-emissive P-rhodamine fluorophores, Org. Biomol. Chem. 18 (2020) 1567-1571.

[46] M. J. Frisch, G. W. Trucks, H. B. Schlegel, G. E. Scuseria, M. A. Robb, J. R. Cheeseman, J. A. Montgomery Jr., T. Vreven, K. N. Kudin, J. C. Burant, J. M. Millam, S. S. Iyengar, J. Tomasi, V. Barone, B. Mennucci, M. Cossi, G. Scalmani, N. Rega, G. A. Petersson, H. Nakatsuji, M. Hada, M. Ehara, K. Toyota, R. Fukuda, J. Hasegawa, M. Ishida, T. Nakajima, Y. Honda, O. Kitao, H. Nakai, M. Klene, X. Li, J. E. Knox, H. P. Hratchian, J. B. Cross, V. Bakken, C. Adamo, J. Jaramillo, R. Gomperts, R. E. Stratmann, O. Yazyev, A. J. Austin, R. Cammi, C. Pomelli, J. W. Ochterski, P. Y. Ayala, K. Morokuma, G. A. Voth, P. Salvador, J. J. Dannenberg, V. G. Zakrzewski, S. Dapprich, A. D. Daniels, M. C. Strain, O. Farkas, D. K. Malick, A. D. Rabuck, K. Raghavachari, J. B. Foresman, J. V. Ortiz, Q. Cui, A. G. Baboul, S. Clifford, J. Cioslowski, B. B. Stefanov, G. Liu, A. Liashenko, P. Piskorz, I. Komaromi, R. L. Martin, D. J. Fox, T. Keith, M. A. Al- Laham, C. Y. Peng, A. Nanayakkara, M. Challacombe, P. M. W. Gill, B. Johnson, W. Chen, M. W. Wong, C. Gonzalez, J. A. Pople, Gaussian 09, Revision A.02, Gaussian, Inc., Wallingford CT, 2009.

[47] T. Lu, F. Chen, Multiwfn: A multifunctional wavefunction analyzer, J. Comput. Chem. 33 (2012) 580-592.

[48] W. Humphrey, A. Dalke, K. Schulten, VMD: visual molecular dynamics, J. Molec. Graphics 14 (1996) 33-38.

F. D. synthesized the compounds. Z. X. supervised the project. F. D., Q. Q. and Z. X. wrote the paper. L

Declaration of interests

☒ The authors declare that they have no known competing financial interests or personal relationships that could have appeared to influence the work reported in this paper.

☐The authors declare the following financial interests/personal relationships which may be considered as potential competing interests:

Graphical abstract

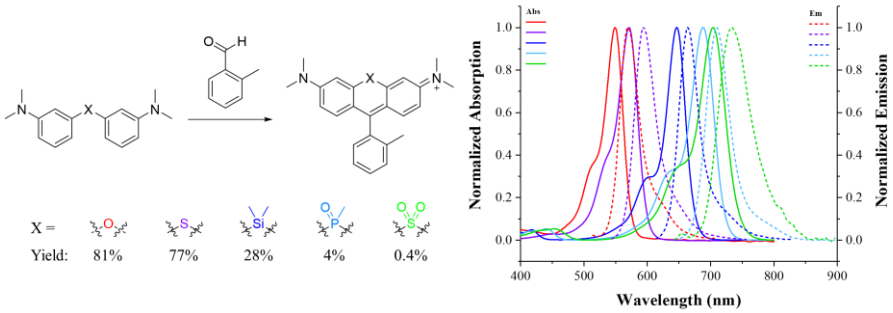

Highlight

1. Five heteroatom-substituted rhodamines through the condensation of diaryl ether analogues and *o*-tolualdehyde were systematically synthesized.
2. The electron-donating moiety increased the nucleophilic ability of diaryl ether analogues and facilitated the condensation reaction.
3. Rhodamines with strong electron-withdrawing moiety in the 10^{th} position hindered the condensation reaction and resulted the poor yield.

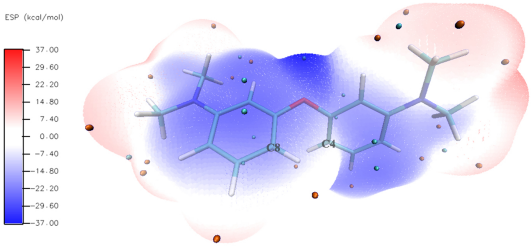

DAEA-O

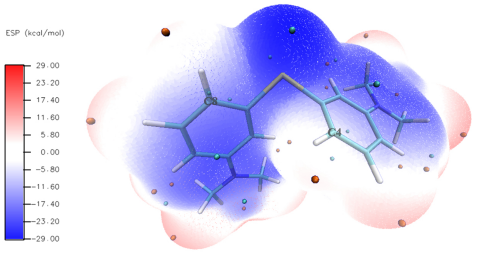

DAEA-S

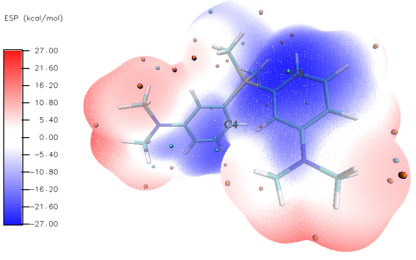

DAEA-Si

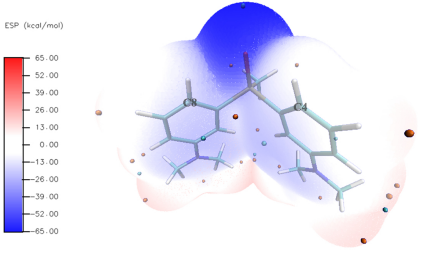

DAEA-PO

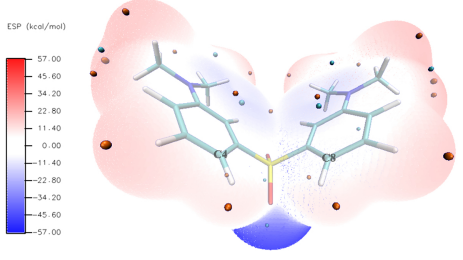

DAEA-SO_2

Figure 1

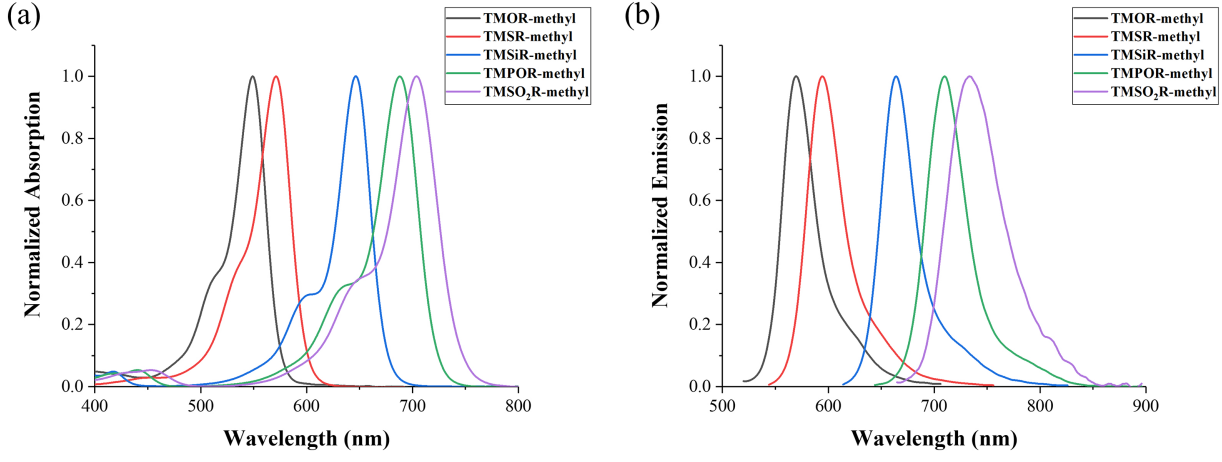
(a)
TMOR-methyl
TMSR-methyl
TMSiR-methyl
TMPOR-methyl
TMSO2R-methyl
Normalized Absorption
Wavelength (nm)
(b)
TMOR-methyl
TMSR-methyl
TMSiR-methyl
TMPOR-methyl
TMSO2R-methyl
Normalized Emission
Wavelength (nm)

Figure 2